

Classification
Physics Abstracts
 05.20

Zero temperature parallel dynamics for infinite range spin glasses and neural networks

E. Gardner ⁽¹⁾, B. Derrida ⁽²⁾ and P. Mottishaw ⁽²⁾

⁽¹⁾ Department of Physics, University of Edinburgh, Edinburgh EH9, 3JZ, U.K.

⁽²⁾ Service de Physique Théorique, CEN Saclay, 91191 Gif-sur-Yvette Cedex, France

(*Reçu le 5 novembre 1986, accepté le 20 janvier 1987*)

Résumé. — Nous présentons les résultats de calculs analytiques et numériques pour une dynamique parallèle à température nulle de modèles de verres de spin et de réseaux de neurones. Nous utilisons une approche analytique pour calculer l'aimantation et les recouvrements après quelques pas de temps. Dans la limite des temps longs, cette approche analytique devient trop compliquée et nous utilisons des méthodes numériques. Pour le modèle de Sherrington-Kirkpatrick, nous mesurons l'aimantation rémanente et les recouvrements à des temps différents et nous observons des décroissances en loi de puissance. Quand on itère deux configurations différentes, leur distance $d(\infty)$ au bout d'un temps infini dépend de leur distance initiale $d(0)$. Nos résultats numériques suggèrent que $d(\infty)$ a une limite finie quand $d(0) \rightarrow 0$. Ce résultat signifie qu'il y a un effet collectif entre un nombre infini de spins. Pour le modèle de Little-Hopfield, nous calculons l'évolution temporelle du recouvrement avec une pattern mémorisée. Nous observons un régime pour lequel le système retient mieux après quelques pas de temps que dans la limite des temps longs.

Abstract. — We present the results of analytical and numerical calculations for the zero temperature parallel dynamics of spin glass and neural network models. We use an analytical approach to calculate the magnetization and the overlaps after a few time steps. For the long time behaviour, the analytical approach becomes too complicated and we use numerical simulations. For the Sherrington-Kirkpatrick model, we measure the remanent magnetization and the overlaps at different times and we observe power law decays towards the infinite time limit. When one iterates two configurations in parallel, their distance $d(\infty)$ in the limit of infinite time depends on their initial distance $d(0)$. Our numerical results suggest that $d(\infty)$ has a finite limit when $d(0) \rightarrow 0$. This result can be regarded as a collective effect between an infinite number of spins. For the Little-Hopfield model, we compute the time evolution of the overlap with a stored pattern. We find regimes for which the system learns better after a few time steps than in the infinite time limit.

1. Introduction.

Zero temperature dynamics have become of more and more interest in the study of spin glasses and of neural networks [1-5, 9, 10, 19]. They exhibit qualitatively the same features (many metastable states, remanence effects) as spin glasses at low temperature. However they are much simpler to study from a theoretical point of view because the effect of thermal noise is eliminated. They may also have practical advantages if one wants to build pattern recognition devices.

The reason that zero temperature dynamics are non-trivial and interesting is the existence of many metastable states [6]. These metastable states are responsible for remanence effects [7], very slow relaxations and sensitivity to initial conditions.

They are also at the origin of all optimization problems [8]. At the moment one knows, at least in infinite ranged models, how to compute the number of metastable states [6, 11]. However much less is known about the sizes and the shapes of their basins of attraction which play a crucial role in zero temperature dynamics [3, 11, 12]. Even the characterization of these sizes and shapes is not easy.

In the present work, we will develop an approach to zero temperature dynamics. This paper will treat only parallel dynamics because it simplifies our calculations but we think that some of our results could be generalized to serial dynamics. We will mainly consider a system of N Ising spins. ($\sigma_i = \pm 1$) with interactions, J_{ij} , between all pairs of distinct spins. The interactions are defined such that

$J_{ij} = J_{ji}$, and $J_{ii} = 0$, but more general cases can be dealt with using the same analytic approach.

Parallel dynamics means that the configurations at time step t is given by the rule

$$\sigma_i^t = \text{sign} \left[\sum_{j=1}^N J_{ij} \sigma_j^{t-1} \right] \quad (1.1)$$

where all the spins are updated at the same time. We consider, the J_{ij} are random variables which remain fixed in time. Therefore for a given sample, and a given initial configuration $\{\sigma_i^0\}$ at time $t = 0$, the configuration at any later time t is uniquely determined by iterating equation (1.1).

We will consider three models. Firstly, the Sherrington-Kirkpatrick [13] spin glass model for which the J_{ij} are independent random variables with a distribution

$$\rho(J_{ij}) = \sqrt{\frac{N}{2\pi J^2}} \exp \left(-\frac{NJ_{ij}^2}{2J^2} \right). \quad (1.2)$$

Secondly, the Little-Hopfield model [14, 15] which is a pattern recognition model. The J_{ij} are given in this model by

$$J_{ij} = \frac{1}{N} \sum_{\mu=1}^{N\alpha} \xi_i^{(\mu)} \xi_j^{(\mu)}, \quad (1.3)$$

where $N\alpha$ is the number of patterns which are stored and $\xi_i^{(\mu)} = \pm 1$ is the value of spin σ_i in the pattern μ .

The third model we consider is a generalization of the Little-Hopfield model to the case of p -spin interactions [16]. The updating rule, equation (1.1), is generalized to

$$\sigma_{j_1}^t = \text{sign} \left[\sum_{j_2 \dots j_p} J_{j_1, j_2, \dots, j_p} \sigma_{j_2}^{t-1} \dots \sigma_{j_p}^{t-1} \right] \quad (1.4)$$

where

$$J_{j_1, j_2, \dots, j_p} = \frac{p!}{N^{p-1}} \sum_{\mu=1}^{2N^{p-1}\alpha/p!} \xi_{j_1}^{(\mu)} \dots \xi_{j_p}^{(\mu)} \quad (1.5)$$

and the number of patterns is $2N^{p-1}\alpha/p!$.

In section 2 we present an analytic approach which allows one to compute the time evolution of magnetization, overlaps, local fields, etc. averaged over disorder, after an arbitrary number of time steps. For the SK model we compute certain quantities exactly up to the 5th time step. Although the method can in principle be used to compute all properties

after an arbitrary number of time steps, in practice the number of order parameters increases very quickly with time and makes each time step more difficult.

In section 3, we apply the same method to the two neural network models. We give the analytic expression of the overlap with a stored pattern after one and two time steps.

In section 4 we present various numerical calculations for the SK and the Little-Hopfield models with parallel zero temperature dynamics.

For the SK model at short times the numerical results agree with the results obtained by the analytic method of section 2. At longer times, these results indicate a power law decrease of magnetization and of the overlap between successive times. The study of the overlap between two configurations show that the basins of attraction of the different valleys have a high degree of interpenetration.

For the Little-Hopfield model, we obtain the projection on a stored pattern after one, two and an infinite number of times steps as a function of the projection at time $t = 0$. Again the results at short times agree with the results of section 3 whereas the results at long time show a clear change between the good recall and the bad recall phases.

2. The SK model.

The map, equation (1.1), is deterministic, so that given an initial spin configuration $\{\sigma_i^0\}$ at $t = 0$, the spin configuration, $\{\sigma_i^t\}$, at any later time, t , is uniquely determined. Consider

$$n_T(\{\sigma_i^0\}, \{\sigma_i^T\}) = \text{Tr}_{\sigma_i^t} \prod_{t=1}^T \prod_{i=1}^N \theta \left(\sigma_i^t \sum_{j=1}^N J_{ij} \sigma_j^{t-1} \right),$$

where

$$\theta(x) = \begin{cases} 1 & \text{if } x > 0 \\ 0 & \text{if } x < 0 \end{cases}.$$

This quantity is unity if $\{\sigma_i^T\}$ is the descendent of $\{\sigma_i^0\}$ after T iterations of the map and zero otherwise. The disorder average of $n_T(\{\sigma_i^0\}, \{\sigma_i^T\})$ is the probability that for a randomly chosen sample, $\{\sigma_i^T\}$ is the descendent of $\{\sigma_i^0\}$ after T time steps. This allows, for example, the average magnetization after T time steps from an initial configuration $\{\sigma_i^0\}$ to be written

$$m(T) = \frac{1}{N} \left\langle \sum_i \sigma_i^T \right\rangle_{\{J_{ij}\}} = \left\langle \text{Tr}_{\sigma_i^t} \left(\frac{1}{N} \sum_i \sigma_i^T \right) \prod_{t=1}^T \prod_{i=1}^N \theta \left(\sigma_i^t \sum_{\substack{j=1 \\ (\neq i)}}^N J_{ij} \sigma_j^{t-1} \right) \right\rangle_{\{J_{ij}\}}, \quad (2.1)$$

where $\langle \rangle_{\{J_{ij}\}}$ denotes an average over the random couplings.

As we will show in this section the natural parameters of the problem are related to the disorder averaged correlation functions between the spins, σ_i^t , and the local fields H_i^t given by

$$y(h(t_1, t_2), g(t_1, t_2)) = \left\langle \text{Tr}_{\sigma_i^t} \left\{ \prod_{t=1,2,\dots,T}^T \prod_{i=1}^N \theta \left(\sigma_i^t \sum_j J_{ij} \sigma_j^{t-1} \right) \times \right. \right. \right. \times \exp \left(\sum_{t_1 t_2} \left[h(t_1, t_2) \sum_i \sigma_i^{t_1} \sigma_i^{t_2} + g(t_1, t_2) \sum_i \sigma_i^{t_1} H_i^{t_2} \right] \right) \left. \right\} \right\rangle_{\{J_{ij}\}} \quad (2.3)$$

so that

$$\frac{\partial y}{\partial h(t_1, t_2)} \Big|_{h, g=0} = \left\langle \sum_i \sigma_i^{t_1} \sigma_i^{t_2} \right\rangle_{\{J_{ij}\}} \quad (2.4a)$$

and

$$\frac{\partial y}{\partial g(t_1, t_2)} \Big|_{h, g=0} = \left\langle \sum_i \sigma_i^{t_1} H_i^{t_2} \right\rangle_{\{J_{ij}\}}. \quad (2.4b)$$

Note that $y(0, 0) = 1$, since for a given initial configuration, the configuration at each later time is uniquely determined. From equation (2.3), $y(g, h)$ is invariant under the gauge transformation $J_{ij} \rightarrow J_{ij} \varepsilon_i \varepsilon_j$, $\sigma_i^t \rightarrow \varepsilon_i \sigma_i^t$ (and therefore $H_i^t \rightarrow \varepsilon_i H_i^t$) for all time $t > 0$. This transformation changes the initial configuration from σ_i^0 to $\varepsilon_i \sigma_i^0$, so that $y(h, g)$ is independent of the initial configuration. For convenience we shall take a normalized trace ($\text{Tr} 1 = 1$) over the initial configuration. Of particular interest is the average magnetization after t time steps, from an initial configuration with all spins up.

$$y(h, g) = \text{Tr}_{\sigma_i^t} \int_{-\infty}^{\infty} \prod_{i,t} \left[\frac{dx_i^t}{2\pi} \right] \int_0^{\infty} \prod_{i,t} [d\lambda_i^t] \exp \left[i \sum_{i,t} \lambda_i^t x_i^t + \sum_{t_1 t_2} h(t_1, t_2) \sum_i \sigma_i^{t_1} \sigma_i^{t_2} \right] Y(\sigma_i^t, x_i^t, g) \quad (2.7)$$

where

$$Y(\sigma_i^t, x_i^t, g) \equiv \left\langle \exp \left\{ -i \sum_{i,t_1} \left(x_i^{t_1} \sigma_i^{t_1} + i \sum_{t_2} g(t_2, t_1) \sigma_i^{t_2} \right) \sum_j J_{ij} \sigma_j^{t_1-1} \right\} \right\rangle_{\{J_{ij}\}}. \quad (2.8)$$

Performing the disorder average, over the distribution $\rho(J_{ij})$ equation (1.2) gives

$$Y(\sigma_i^t, x_i^t, g) = \exp \left\{ -\frac{J^2}{2N} \sum_{i < j} \left(\sum_{t_1=1}^T \left[\left(x_i^{t_1} \sigma_i^{t_1} + i \sum_{t_2} g(t_2, t_1) \sigma_i^{t_2} \right) \sigma_j^{t_1-1} + \left(x_j^{t_1} \sigma_j^{t_1} + i \sum_{t_2} g(t_2, t_1) \sigma_j^{t_2} \right) \sigma_i^{t_1-1} \right] \right)^2 \right\}. \quad (2.9)$$

Retaining terms of leading order in N , in the exponent, this can be written

$$Y(\sigma_i^t, x_i^t, g) = \exp \left\{ -\frac{J^2}{2N} \sum_{t_1=1}^T \sum_{t_2=1}^T \left[\left(\sum_i \left(x_i^{t_1} \sigma_i^{t_1} + i \sum_{t_3} g(t_3, t_1) \sigma_i^{t_3} \right) \left(x_i^{t_2} \sigma_i^{t_2} + i \sum_{t_4} g(t_4, t_2) \sigma_i^{t_4} \right) \right) \times \left(\sum_j \sigma_j^{t_1-1} \sigma_j^{t_2-1} \right) + \left(\sum_i \left(x_i^{t_1} \sigma_i^{t_1} + i \sum_{t_3} g(t_3, t_1) \sigma_i^{t_3} \right) \sigma_i^{t_2-1} \right) \left(\sum_j \left(x_j^{t_2} \sigma_j^{t_2} + i \sum_{t_4} g(t_4, t_1) \sigma_j^{t_4} \right) \sigma_j^{t_1-1} \right) \right] \right\}. \quad (2.10)$$

$$H_i^t = \sum_j J_{ij} \sigma_j^{t-1} \quad (2.2)$$

at different times. These can be computed from the following generating functional,

This is given by

$$m(t) \equiv \left\langle \frac{1}{N} \sum_i \sigma_i^t \right\rangle_{\{J_{ij}\}} = \frac{1}{N} \frac{\partial y}{\partial h(0, t)}. \quad (2.5)$$

$m(t)$, given by (2.5) is the magnetization after t time steps if one starts with $m(0) = 1$. For any other starting configuration $m(t)$ is the projection of the configuration at time t on the configuration at time 0. If one starts at $t = 0$ with a configuration with magnetization μ , then at time t , the magnetization will be $\mu m(t)$.

In order to perform the averages over the random couplings J_{ij} , we will use the following integral representation of the θ functions, in equation (2.3),

$$\theta(R_i^t) = \int_{-\infty}^{\infty} \frac{dx_i^t}{2\pi} \int_0^{\infty} d\lambda_i^t e^{ix_i^t(\lambda_i^t - R_i^t)} \quad (2.6)$$

where $R_i^t = \sigma_i^t \sum_j J_{ij} \sigma_j^{t-1}$. Thus

The first term in the exponent can be reduced to a single sum over sites by introducing the delta function constraint

$$\begin{aligned} \int_{-\infty}^{\infty} \prod_{t_1 < t_2} \left[N \, dq^{t_1 t_2} \frac{dp^{t_1 t_2}}{2 \pi} \exp \left\{ i \left(N q^{t_1 t_2} p^{t_1 t_2} - p^{t_1 t_2} \sum_i \sigma_i^{t_1-1} \sigma_i^{t_2-1} \right) \right\} \right] = \\ = \int \prod_{t_1 < t_2} \left[N \, dq^{t_1 t_2} \delta \left(N q^{t_1 t_2} - \sum_i \sigma_i^{t_1-1} \sigma_i^{t_2-1} \right) \right] = 1. \quad (2.11) \end{aligned}$$

Similarly the second term in the exponent of equation (2.10) can be decoupled using Gaussian integral identities. The result is

$$\begin{aligned} Y(\sigma_i^t, x_i^t, g) = \text{Const.} \int \prod_{t_1 < t_2} dq^{t_1 t_2} dp^{t_1 t_2} \int \prod_{t_1 \neq t_2} ds^{t_1 t_2} \times \\ \times \int \prod_t dr^t \exp \left\{ N \left[i \sum_{t_1 < t_2} q^{t_1 t_2} p^{t_1 t_2} - \frac{1}{2 J^2} \sum_{t_1 \neq t_2} s^{t_1 t_2} s^{t_2 t_1} - \frac{J^2}{2} \sum_t (r^t)^2 \right] \right\} \\ \times \prod_{i=1}^N \exp \left\{ -i \sum_{t_1 < t_2} p^{t_1 t_2} \sigma_i^{t_1-1} \sigma_i^{t_2-1} - i \sum_{t_1 \neq t_2} s^{t_1 t_2} \left(x_i^{t_1} \sigma_i^{t_1} \sigma_i^{t_2-1} + i \sum_{t_3} g(t_3, t_1) \sigma_i^{t_3} \sigma_i^{t_2-1} \right) \right. \\ \left. - \frac{J^2}{2} \sum_{t_1 \neq t_2} q^{t_1 t_2} \left(x_i^{t_1} \sigma_i^{t_1} + i \sum_{t_3} g(t_3, t_1) \sigma_i^{t_3} \right) \left(x_i^{t_2} \sigma_i^{t_2} + i \sum_{t_4} g(t_4, t_2) \sigma_i^{t_4} \right) \right. \\ \left. - \frac{J^2}{2} \sum_{t_1} \left(x_i^{t_1} \sigma_i^{t_1} + i \sum_{t_2} g(t_2, t_1) \sigma_i^{t_2} \right)^2 + i J^2 \sum_{t_1} r^{t_1} \left(x_i^{t_1} \sigma_i^{t_1} \sigma_i^{t_1-1} + i \sum_{t_2} g(t_2, t_1) \sigma_i^{t_2} \sigma_i^{t_1-1} \right) \right\} \quad (2.12) \end{aligned}$$

where the Const. depends only on N and J and plays no role in the following because we use a saddle point calculation.

Thus $y(h, g)$, equation (2.7), can be written as an integral over the variables $p^{t_1 t_2}$, $q^{t_1 t_2}$, r^t , $s^{t_1 t_2}$; which can be computed by steepest descents in the limit $N \rightarrow \infty$.

$$y(h, g) = \text{Const.} \int_{-\infty}^{\infty} \prod_{t_1 < t_2} [dq^{t_1 t_2} dp^{t_1 t_2}] \prod_{t_1 \neq t_2} [ds^{t_1 t_2}] \prod_t [dr^t] \exp NF(q^{t_1 t_2}, p^{t_1 t_2}, s^{t_1 t_2}, r^t, g, h) \quad (2.13a)$$

where

$$F(q, p, s, r, g, h) = i \sum_{t_1 < t_2} p^{t_1 t_2} q^{t_1 t_2} - \frac{1}{2 J^2} \sum_{t_1 \neq t_2} s^{t_1 t_2} s^{t_2 t_1} - \frac{J^2}{2} \sum_t (r^t)^2 + \ln \tilde{y}(q, p, s, r, g, h) \quad (2.13b)$$

and

$$\begin{aligned} \tilde{y}(q, p, s, r, g, h) = \text{Tr} \int_0^{\infty} d\lambda^t \int_{-\infty}^{\infty} \frac{dx^t}{2 \pi} \exp \left\{ +i \sum_t x^t \lambda^t - \frac{J^2}{2} \sum_{t_1} \left(x^{t_1} \sigma^{t_1} + i \sum_{t_2} g(t_2, t_1) \sigma^{t_2} \right)^2 \right. \\ \left. - \frac{J^2}{2} \sum_{t_1 \neq t_2} q^{t_1 t_2} \left(x^{t_1} \sigma^{t_1} + i \sum_{t_3} g(t_3, t_1) \sigma^{t_3} \right) \left(x^{t_2} \sigma^{t_2} + i \sum_{t_4} g(t_4, t_2) \sigma^{t_4} \right) \right. \\ \left. + i J^2 \sum_{t_1} r^{t_1} \left(x^{t_1} \sigma^{t_1} \sigma^{t_1-1} + i \sum_{t_2} g(t_2, t_1) \sigma^{t_2} \sigma^{t_1-1} \right) - i \sum_{t_1 < t_2} p^{t_1 t_2} \sigma^{t_1-1} \sigma^{t_2-1} \right. \\ \left. - i \sum_{t_1 \neq t_2} s^{t_1 t_2} \left(x^{t_1} \sigma^{t_1} \sigma^{t_2-1} + i \sum_{t_3} g(t_3, t_1) \sigma^{t_3} \sigma^{t_2-1} \right) + \sum_{t_1 t_2} h(t_1, t_2) \sigma^{t_1} \sigma^{t_2} \right\} \quad (2.13c) \end{aligned}$$

In all the sums the upper limit is T and the lower limit is 1. The saddle point equations are for $g(t_i, t_j) = 0$ and $h(t_i, t_j) = 0$

$$q^{t_1 t_2} = \langle \sigma^{t_1-1} \sigma^{t_2-1} \rangle_{\tilde{y}}$$

$$\begin{aligned} ip^{t_1 t_2} &= J^2 \langle x^{t_1} x^{t_2} \sigma^{t_1} \sigma^{t_2} \rangle_{\tilde{y}} \\ is^{t_1 t_2} &= J^2 \langle x^{t_2} \sigma^{t_2} \sigma^{t_1-1} \rangle_{\tilde{y}} \\ r^t &= i \langle x^t \sigma^t \sigma^{t-1} \rangle_{\tilde{y}} \end{aligned} \quad (2.14a)$$

where the expectation value $\langle \dots \rangle_y$ is with respect to the generalized trace defined in equation (2.13c), with $h(t_1, t_2) = 0$ and $g(t_1, t_2) = 0$, i.e. with

$$\begin{aligned} \tilde{y}(q, p, s, p, r, o, o) = \text{Tr}_{\sigma^t} \int_0^\infty d\lambda^t \int_{-\infty}^{+\infty} \frac{dx^t}{2\pi} \exp \left\{ +i \sum_t x^t \lambda^t - \frac{J^2}{2} \sum_{t_1} x_{t_1}^2 - \frac{J^2}{2} \sum_{t_1 \neq t_2} q^{t_1 t_2} x^{t_1} \sigma^{t_1} x^{t_2} \sigma^{t_2} \right. \\ \left. + i J^2 \sum_{t_1} r^{t_1} x^{t_1} \sigma^{t_1} \sigma^{t_1-1} - i \sum_{t_1 < t_2} p^{t_1 t_2} \sigma^{t_1-1} \sigma^{t_2-1} - i \sum_{t_1 \neq t_2} s^{t_1 t_2} x^{t_1} \sigma^{t_1} \sigma^{t_2-1} \right\}. \end{aligned} \quad (2.14b)$$

A useful check on the saddle point equations, is that in zero field the exponent in (2.13a) should vanish as $y(0, 0) = 1$ from equation (2.3).

A direct evaluation of these expectation values in zero field ($h = y = 0$), (see Appendix 1 for details) show that a number of order parameters vanish :

$$\begin{aligned} p^{t_1 t_2} &= 0 & \text{for all } t_1, t_2 \\ r^t &= 0 & \text{for all } t \\ s^{t_1 t_2} &= 0 & \text{if } t_2 > t_1. \end{aligned} \quad (2.15)$$

The physical meaning of the order parameters can be obtained by taking derivatives of equation (2.13a) with respect to $h(t_1, t_2)$ and $g(t_1, t_2)$ and comparing with equations (2.4). The derivative with respect to h gives

$$q^{t_1 t_2} = \left\langle \frac{1}{N} \sum_i \sigma_i^{t_1-1} \sigma_i^{t_2-1} \right\rangle_{\{J_{ij}\}} \quad (2.16)$$

where $q^{t_1 t_2}$ is evaluated in zero field. Thus $q^{t_1 t_2}$ is equal to the overlap between configurations at time $t_1 - 1$ and $t_2 - 1$. If one makes the global change $\{J_{ij}\} \rightarrow \{-J_{ij}\}$, the dynamics (1.1) of the spins implies that $\sigma_i^t \rightarrow -\sigma_i^t$ for odd t and $\sigma_i^t \rightarrow \sigma_i^t$ for even t . Therefore since the distribution of J_{ij} is symmetric, one has

$$q^{t_1 t_2} = 0 \quad \text{for } |t_1 - t_2| \text{ odd} \quad (2.17)$$

This is certainly true for all times t_1 and t_2 with $|t_1 - t_2|$ odd, but we did not find how to derive it easily from the saddle point equations.

Taking the derivative of equation (2.14b) with respect to g , gives

$$\begin{aligned} \left\langle \frac{1}{N} \sum_i \sigma_i^{t_1-1} H_i^{t_2} \right\rangle_{\{J_{ij}\}} &= \\ &= s^{t_2 t_1} + \sum_{t_3=1}^T s^{t_2 t_3} q^{t_1 t_3} + \sum_{\substack{t_3=1 \\ (\neq t_1, t_2)}}^T q^{t_2 t_3} s^{t_1 t_3} \end{aligned} \quad (2.18)$$

where $t_2 < t_1$ and equations (2.15) have been used. Due to the symmetric distribution of the J_{ij} 's, the left hand side of equation (2.17) vanishes when $|t_1 - t_2|$ is even, so that

$$s^{t_1 t_2} = 0 \quad \text{for all } |t_1 - t_2| \text{ even.} \quad (2.19)$$

We will now consider the time evolution of the average magnetization starting from an initial configuration with magnetization 1. Setting $t_1 = 1$ in equation (2.16) gives for the average magnetization after t time steps

$$m(t) = q^{1, t+1}. \quad (2.20)$$

If one wants to know the properties of the system at time t , it is clear that one does not need to know what happens at later times $t' > t$. Therefore the order parameters defined at a particular pair of time steps can depend only on parameters defined at previous time steps. Thus at short times the properties of the model are determined by a few order parameters. At successive time steps the number of order parameters increases rapidly (approximately as the square of the time).

The equations obtained from the saddle point for the remanent magnetization after two time steps are

$$\begin{aligned} s^{21} &= \sqrt{\frac{2}{\pi}} \\ s^{32} &= \sqrt{\frac{2}{\pi}} e^{-(s^{21})^2/2} \\ m(2) &= q^{13} = 2 \operatorname{erf}(s^{21}) \end{aligned} \quad (2.21)$$

where

$$\operatorname{erf}(x) \equiv \frac{1}{\sqrt{2\pi}} \int_0^x dy e^{-y^2/2}.$$

The equations for the order parameters and magnetization upto $T = 4$ are given in appendix 2.

Using equations (2.21), (2.16), (2.18) and the results of appendix 2 we obtain for the first few order parameters,

$$\begin{aligned} \langle H^2 \rangle &= \langle H^2 \sigma^0 \rangle = 0.748 \\ \langle H^4 \sigma^2 \rangle &= 1.141 \\ \langle H^3 \sigma^1 \rangle &= 1.039 \\ \langle H^5 \sigma^3 \rangle &= 1.197 \\ \langle H^4 \rangle &= \langle H^4 \sigma^0 \rangle = 0.681 \\ \langle H^5 \sigma^1 \rangle &= 1.012 \\ m(2) &= q^{13} = 0.575 \\ q^{24} &= 0.760 \\ q^{35} &= 0.835 \\ m(4) &= q^{15} = 0.468 \end{aligned} \quad (2.22)$$

since $m(t)$ vanishes for odd values of t the magnetization oscillates between zero and a finite value which decreases with time. Clearly its value at successive time steps provides one way of approximating the final remanent magnetization.

Numerical results to be described in section 4 show that the final value is 0.23 ± 0.02 so the approximate value $m(4) = 0.468$ is still rather far from the correct one.

3. Neural network models.

In this section we show how the properties of the Little model, equation (1.3), and its p-spin generalization, equations (1.4), (1.5) can be obtained analytically. The method is similar to that used for the SK model in section 2.

In the Little-Hopfield model $N\alpha$ patterns are chosen at random, thus the overlap between two patterns is typically of order $N^{-1/2}$. In the $N \rightarrow \infty$ limit this overlap is zero and the patterns are

orthogonal. We consider spin configurations which have a finite overlap with one of the patterns, and a microscopic overlap (of order $N^{-1/2}$) with the remaining patterns. The overlap between a given pattern $\{\xi_i^{(\mu)}\}$ and the spin configuration $\{\sigma_i^t\}$ at time t is defined by

$$m_\mu^t = \frac{1}{N} \sum_{i=1}^N \sigma_i^t \xi_i^{(\mu)}. \quad (3.1)$$

The time evolution of m_μ^t depends strongly on the choice of the initial spin configuration at $t = 0$. Here we shall choose the initial spin configuration to have a finite overlap with the $\mu = 1$ pattern, and a microscopic overlap with the remaining patterns. We assume that this property holds for the subsequent spin configuration in time. This assumption is shown to be self consistent, at least for short times.

A generating functional for the average spin-spin correlation function can be defined in the same way as for the SK model :

$$y(h_{t_1 t_2}) = \left\langle \text{Tr}'_{\sigma_i^0} \text{Tr}_{\sigma_i^t} \left[\prod_{i=1}^N \prod_{t=1}^T \theta \left(\sigma_i^t \sum_{j=1}^N J_{ij} \sigma_j^{t-1} \right) \exp \left(\sum_{t_1 t_2} h_{t_1 t_2} \sum_i \sigma_i^{t_1} \sigma_i^{t_2} \right) \right] \right\rangle_{\{\xi_i^\mu\}} \quad (3.2)$$

where $\langle \rangle_{\{\xi_i^\mu\}}$ indicates an average over all the $N\alpha$ patterns. The trace, Tr' over the initial spin configuration is restricted to

$$\sigma_i^0 = \begin{cases} \xi_i^1 & 1 \leq i \leq Ng \\ -\xi_i^1 & Ng < i \leq N \end{cases}, \quad (3.3)$$

so that it has overlap $2g - 1$ with the $\mu = 1$ pattern. Introducing the integral representation, equation (2.6), for the θ -functions, y becomes

$$y(h_{t_1 t_2}) = \left\langle \text{Tr}'_{\sigma_i^0} \text{Tr}_{\sigma_i^t} \exp \left(\sum_{t_1 t_2} h_{t_1 t_2} \sum_i \sigma_i^{t_1} \sigma_i^{t_2} \right) \prod_{i,t} \left[\int_0^\infty d\lambda_i^t \int_{-\infty}^\infty \frac{dx_i^t}{2\pi} \times \right. \right. \\ \left. \left. \times \exp \left\{ i\lambda_i^t x_i^t - \frac{i}{N} \sum_{\mu=1}^{N\alpha} x_i^t \sigma_i^t \xi_i^\mu \left(\sum_j \xi_j^\mu \sigma_j^{t-1} \right) + i\alpha x_i^t \sigma_i^t \sigma_i^{t-1} \right\} \right] \right\rangle \quad (3.4)$$

In order to perform the average over the patterns we use the identity

$$1 \equiv \prod_{\mu,t} \left[\int_{-\infty}^\infty N dm_\mu^{t-1} \int_{-\infty}^\infty \frac{dn_\mu^{t-1}}{2\pi} \exp \left(iNn_\mu^{t-1} m_\mu^{t-1} - in_\mu^{t-1} \sum_{i=1}^N \sigma_i^{t-1} \xi_i^\mu \right) \right], \quad (3.5)$$

so that y becomes,

$$y(h_{t_1 t_2}) = \int_{-\infty}^\infty \left[N dm_\mu^{t-1} \frac{dn_\mu^{t-1}}{2\pi} \right] e^{iN \sum_{\mu,t} n_\mu^{t-1} m_\mu^{t-1}} \left\langle \text{Tr}'_{\sigma_i^0} \text{Tr}_{\sigma_i^t} \int_0^\infty [d\lambda_i^t] \int_{-\infty}^\infty \left[\frac{dx_i^t}{2\pi} \right] e^{i \sum_{i,t} \lambda_i^t x_i^t} \times \right. \\ \left. \times \exp \left(i\alpha \sum_{i,t} x_i^t \sigma_i^t \sigma_i^{t-1} + \sum_{t_1 t_2} h_{t_1 t_2} \sum_i \sigma_i^{t_1} \sigma_i^{t_2} - i \sum_t n_t^{t-1} \sum_i \sigma_i^{t-1} \xi_i^1 - i \sum_t m_t^{t-1} \sum_i x_i^t \sigma_i^t \xi_i^1 \right) \right. \\ \left. \times Y(x_i^t, \sigma_i^t, m_\mu^t, n_\mu^t) \right\rangle_{\xi_i^1} \quad (3.6)$$

where

$$Y(x_i^t, \sigma_i^t, m_\mu^t, n_\mu^t)_{(\mu \neq 1)} = \exp \left\{ \sum_{\mu=2}^{N\alpha} \sum_i \ln \left(\cos \left[\sum_{t=1}^T (n_\mu^{t-1} \sigma_i^{t-1} + m_\mu^{t-1} x_i^t \sigma_i^t) \right] \right) \right\}. \quad (3.7)$$

Using the assumption that the spin configuration has a finite overlap only with pattern 1, only the first term in the expansion of $\ln \cos [\cdot]$ contributes to leading order in N . Thus $Y(x_i^t, \sigma_i^t, m_\mu^t, n_\mu^t)$ becomes

$$Y(x_i^t, \sigma_i^t, m_\mu^t, n_\mu^t) = \exp \left\{ -\frac{1}{2} \sum_{t_1 t_2} \left[\left(\sum_{\mu > 1} n_\mu^{t_1-1} n_\mu^{t_2-1} \right) \left(\sum_i \sigma_i^{t_1-1} \sigma_i^{t_2-1} \right) + 2 \left(\sum_{\mu > 1} n_\mu^{t_2-1} m_\mu^{t_1-1} \right) \left(\sum_i x_i^{t_2} \sigma_i^{t_1} \sigma_i^{t_1-1} \right) + \left(\sum_{\mu > 1} m_\mu^{t_1-1} m_\mu^{t_2-1} \right) \left(\sum_i x_i^{t_1} x_i^{t_2} \sigma_i^{t_1} \sigma_i^{t_2} \right) \right] \right\}. \quad (3.8)$$

The sums on sites and sums on patterns can be decoupled by using the identities

$$\begin{aligned} 1 &= \prod_{t_1 < t_2} \left[\int_{-\infty}^{\infty} N\alpha \, dr^{t_1 t_2} \frac{dq^{t_1 t_2}}{2\pi} \exp \left(i\alpha N r^{t_1 t_2} q^{t_1 t_2} - Ni q^{t_1 t_2} \sum_{\mu > 1} n_\mu^{t_1-1} n_\mu^{t_2-1} \right) \right], \\ 1 &= \prod_{t_1, t_2} \left[\int_{-\infty}^{\infty} N\alpha \, dk^{t_1 t_2} \frac{ds^{t_1 t_2}}{2\pi} \exp \left(i\alpha N k^{t_1 t_2} s^{t_1 t_2} - Nis^{t_1 t_2} \sum_{\mu > 1} m_\mu^{t_1-1} n_\mu^{t_2-1} \right) \right], \\ 1 &= \prod_{t_1 \leq t_2} \left[\int_{-\infty}^{\infty} N\alpha \, dl^{t_1 t_2} \frac{dp^{t_1 t_2}}{2\pi} \exp \left(i\alpha N l^{t_1 t_2} p^{t_1 t_2} - Nip^{t_1 t_2} \sum_{\mu > 1} m_\mu^{t_1-1} m_\mu^{t_2-1} \right) \right]. \end{aligned}$$

The final form for $y(h_{t_1 t_2})$ is then

$$y(h_{t_1 t_2}) \propto \int_{-\infty}^{\infty} dm_1^{t-1} dn_1^{t-1} dr^{t_1 t_2} dq^{t_1 t_2} dk^{t_1 t_2} ds^{t_1 t_2} dl^{t_1 t_2} dp^{t_1 t_2} e^{NF(m_1, n_1, \dots, h_{t_1 t_2})} \quad (3.9a)$$

where

$$\begin{aligned} F(m_1^t, n_1^t, \dots, h) &= i\alpha \sum_{t_1 < t_2} r^{t_1 t_2} q^{t_1 t_2} + i\alpha \sum_{t_1 t_2} k^{t_1 t_2} s^{t_1 t_2} + i\alpha \sum_{t_1 \leq t_2} l^{t_1 t_2} p^{t_1 t_2} + \\ &+ i \sum_t n_1^{t-1} m_1^{t-1} + \alpha \ln W(q^{t_1 t_2}, s^{t_1 t_2}, p^{t_1 t_2}) + g \ln \tilde{Z}_+(n_1^t, m_1^t, r^{t_1 t_2}, k^{t_1 t_2}, l^{t_1 t_2}, h^{t_1 t_2}) \\ &+ (1-g) \ln \tilde{Z}_-(n_1^t, m_1^t, r^{t_1 t_2}, k^{t_1 t_2}, l^{t_1 t_2}, h^{t_1 t_2}) \end{aligned} \quad (3.9b)$$

and

$$\begin{aligned} W(q^{t_1 t_2}, s^{t_1 t_2}, p^{t_1 t_2}) &= \int_{-\infty}^{\infty} \prod_{t=1}^T \left[N \, dm^{t-1} \frac{dn^{t-1}}{2\pi} \right] \exp \left\{ iN \sum_t n^{t-1} m^{t-1} - \frac{N}{2} \sum_t (n^{t-1})^2 - \right. \\ &\quad \left. - iN \sum_{t_1 < t_2} q^{t_1 t_2} n^{t_1-1} n^{t_2-1} - iN \sum_{t_1 t_2} s^{t_1 t_2} m^{t_1-1} n^{t_2-1} - iN \sum_{t_1 \leq t_2} p^{t_1 t_2} m^{t_1-1} m^{t_2-1} \right\} \end{aligned} \quad (3.9c)$$

and

$$\begin{aligned} \tilde{Z}_{\pm}(n_1^t, m_1^t, r^{t_1 t_2}, k^{t_1 t_2}, l^{t_1 t_2}, h^{t_1 t_2}) &= \frac{1}{2} \sum_{\sigma_1} \text{Tr}_{\sigma_1} \int_0^{\infty} \prod_{t=1}^T [\, d\lambda^t \,] \int_{-\infty}^{\infty} \prod_{t=1}^T \left[\frac{dx^t}{2\pi} \right] \times \\ &\times \exp \left\{ i \sum_{t=1}^T x^t \lambda^t + i\alpha \sum_{t=1}^T x^t \sigma^t \sigma^{t-1} + \sum_{t_1 t_2} h^{t_1 t_2} \sigma^{t_1} \sigma^{t_2} - \alpha \sum_{t_1 < t_2} r^{t_1 t_2} \sigma^{t_1-1} \sigma^{t_2-1} - \alpha \sum_{t_1 t_2} k^{t_1 t_2} x^{t_1} \sigma^{t_1} \sigma^{t_2-1} \right. \\ &\left. - \frac{\alpha}{2} \sum_{t_1 t_2} l^{t_1 t_2} x^{t_1} x^{t_2} \sigma^{t_1} \sigma^{t_2} \mp i\sigma^0 \sum_{t=1}^T n_1^{t-1} \sigma^{t-1} \mp i\sigma^0 \sum_{t=1}^T m_1^{t-1} x^t \sigma^t \right\}. \end{aligned} \quad (3.9d)$$

The integral in equation (3.9a) can now be computed in the limit $N \rightarrow \infty$ by steepest descents. The saddle point equations are

$$\begin{aligned}
 iq^{t_1 t_2} &= g \langle \sigma^{t_1-1} \sigma^{t_2-1} \rangle_{\tilde{Z}_+} + \\
 &\quad + (1-g) \langle \sigma^{t_1-1} \sigma^{t_2-1} \rangle_{\tilde{Z}_-} \\
 is^{t_1 t_2} &= g \langle x^{t_1} \sigma^{t_1} \sigma^{t_2-1} \rangle_{\tilde{Z}_+} + \\
 &\quad + (1-g) \langle x^{t_1} \sigma^{t_1} \sigma^{t_2-1} \rangle_{\tilde{Z}_-} \\
 ip^{t_1 t_2} &= g \langle x^{t_1} x^{t_2} \sigma^{t_1} \sigma^{t_2} \rangle_{\tilde{Z}_+} + \\
 &\quad + (1-g) \langle x^{t_1} x^{t_2} \sigma^{t_1} \sigma^{t_2} \rangle_{\tilde{Z}_-} \\
 ip^t &= \frac{g}{2} \langle (x^t)^2 \rangle_{\tilde{Z}_+} + \frac{(1-g)}{2} \langle (x^t)^2 \rangle_{\tilde{Z}_-} \\
 m_1^t &= g \langle \sigma^0 \sigma^t \rangle_{\tilde{Z}_+} - (1-g) \langle \sigma^0 \sigma^t \rangle_{\tilde{Z}_-} \\
 n_1^t &= g \langle \sigma^0 x^{t+1} \sigma^{t+1} \rangle_{\tilde{Z}_+} - \\
 &\quad - (1-g) \langle \sigma^0 x^{t+1} \sigma^{t+1} \rangle_{\tilde{Z}_-} \quad (3.10)
 \end{aligned}$$

where the expectation value $\langle \quad \rangle_{\tilde{Z}_\pm}$ is with respect to the weight in equation (3.9d), and

$$\begin{aligned}
 r^{t_1 t_2} &= N \langle n^{t_1-1} n^{t_2-1} \rangle_w \\
 k^{t_1 t_2} &= N \langle m^{t_1-1} m^{t_2-1} \rangle_w \\
 l^{t_1 t_2} &= N \langle m^{t_1-1} m^{t_2-1} \rangle_w, \quad (3.11)
 \end{aligned}$$

where the expectation value $\langle \quad \rangle_w$ is with respect to the weight in equation (3.9c).

The parameters in equation (3.10) are related to correlation functions involving local fields and spins in similar way to the SK parameters in section 2. All the correlation functions are of course always real but due to our definition of the order parameters in the present section some order parameters are imaginary. Using a similar argument to that of appendix 1 we find that certain order parameters are zero :

$$\begin{aligned}
 s^{t_1 t_2} &= 0 \quad \text{for} \quad t_1 \geq t_2 \\
 p^{t_1 t_2} &= 0 \quad \text{for all} \quad t_1, t_2 \\
 n_1^t &= 0 \quad \text{for all} \quad t. \quad (3.12)
 \end{aligned}$$

The non-zero parameters have the following physical interpretation ; $q^{t_1 t_2}$ is the overlap between spin configuration at time $t_1 - 1$ and $t_2 - 1$; $s^{t_1 t_2}$ is related to the overlap of local fields and spins (cf. Eq. (2.18)) and m_1^t is the overlap between pattern 1 and the spin configuration at time t .

The parameters in equation (3.11) are related to the average of the products of the overlaps between

the spin configurations and the patterns with $\mu > 1$. Using the results, equation (3.12), and an argument similar to that given in appendix 1, we find

$$\begin{aligned}
 r^{t_1 t_2} &= 0 \quad \text{for all} \quad t_1, t_2 \\
 k^{t_1 t_2} &= 0 \quad \text{for} \quad t_1 < t_2. \quad (3.13)
 \end{aligned}$$

We have computed the parameters for the first two time step ($T = 2$). Note that the initial overlap is $m_1^0 = 2g - 1$, as it must from the constraint equation (3.3). The non-zero order parameters after one time step are

$$\begin{aligned}
 k^{11} &= i \\
 l^{11} &= 1 \\
 m_1^1 &= 2 \operatorname{erf} \left(\frac{m_1^0}{\sqrt{\alpha}} \right). \quad (3.14)
 \end{aligned}$$

The new non-zero order parameters after two time steps are

$$\begin{aligned}
 iq^{12} &= m_1^0 m_1^1 \\
 s^{12} &= \sqrt{\frac{2}{\pi \alpha}} e^{-(m_1^0)^2/2\alpha} \\
 l^{22} &= 1 + (s^{12})^2 + 2iq^{12}s^{12} \\
 l^{12} &= -iq^{12} - s^{12} \\
 k^{22} &= i \\
 k^{21} &= is^{12} \\
 m_1^2 &= (1 + m_1^0) \operatorname{erf} \left(\frac{m_1^1 - \alpha i k^{21}}{\sqrt{\alpha l^{22}}} \right) + \\
 &\quad + (1 - m_1^0) \operatorname{erf} \left(\frac{m_1^1 + \alpha i k^{21}}{\sqrt{\alpha l^{22}}} \right). \quad (3.15)
 \end{aligned}$$

The qualitative behaviour of the overlap m_1^1 with a stored pattern after one time step (Eq. (3.14)) is different depending on whether α is greater than or less than $\alpha_0 = 2/\pi \approx 0.64$; for α greater than this value m_1^1 is always less than m_1^0 whereas for $\alpha < \alpha_0$, there is a fixed point of equation (2.14) at $m = m_0(\alpha)$; m decreases if $m > m_0(\alpha)$ and increases if $m < m_0(\alpha)$. The transition at α_0 is second order since $m_0(\alpha) \rightarrow 0$ as $\alpha \rightarrow \alpha_0$. Similarly, equation (3.15) implies that m_1^2 increases after the second time step if its starting value m_1^0 is sufficiently small and if $\alpha < 0.67$.

Physically, this means that the system goes towards a learned pattern after one (two) time steps provided $\alpha < 0.64$ (0.67). These values of α are much larger than the value suggested by thermodynamic calculations [9, 20] which predict the existence of an energy valley correlated with the input pattern only if $\alpha < \alpha_c \sim 0.14$. The transition at α_c is first order ; m jumps from zero for $\alpha > \alpha_c$ to a non-zero value.

However the α_c predicted by thermodynamic

calculations may not be relevant to dynamics. Moreover, we will see in section 4 that the critical α for parallel dynamics in the long time limit is clearly smaller than 0.67.

The calculations for multiconnected neural network model can be done in a similar way to the calculations for the Little-Hopfield model. The analogue of equation (3.4) is for $h_{i_1 i_2} = 0$,

$$y = \text{Tr}' \text{Tr} \prod_{\sigma_i^0 \sigma_i^t} \left[\int_0^\infty d\lambda^t \int_{-\infty}^\infty \frac{dx_i^t}{2\pi} e^{i\lambda^t x_i^t} \exp \left(-i \frac{p!}{N^{p-1}} \sum_i \sum_{\mu=1}^{\frac{2N^{p-1}\alpha}{p!}} x_i^t \sigma_i^t \xi_i^\mu \sum_{i_2 < \dots < i_p} \xi_{i_2}^\mu \dots \xi_{i_p}^\mu \sigma_{i_2}^{t-1} \dots \sigma_{i_p}^{t-1} \right) \right]. \quad (3.16)$$

The p spin calculations however turn out to be simpler than the two-spin calculations because correlations between different $J_{i_1 \dots i_p}$ arise only from the symmetry of the interactions [16]. The reason is as

$$\begin{aligned} \left\langle \exp \left(-i \frac{p!}{N^{p-1}} \sum_{i,t} x_i^t \sigma_i^t \xi_i^\mu \sum_{i_2 < \dots < i_p} \xi_{i_2}^\mu \dots \xi_{i_p}^\mu \sigma_{i_2}^{t-1} \dots \sigma_{i_p}^{t-1} \right) \right\rangle = 1 - \frac{1}{2} \left(\frac{p!}{N^{p-1}} \right)^2 \times \\ \times \left\{ \sum_{i_1, i_2} \left(\sum_i x_i^{t_1} \sigma_i^{t_1} x_i^{t_2} \sigma_i^{t_2} \right) \left(\sum_j \sigma_j^{t_1-1} \sigma_j^{t_2-1} \right)^{p-1} \frac{1}{(p-1)!} + \sum_{i_1, i_2} \left(\sum_i x_i^{t_1} \sigma_i^{t_1} \sigma_i^{t_2-1} \right) \right. \\ \left. \times \left(\sum_j x_j^{t_2} \sigma_j^{t_2} \sigma_j^{t_1-1} \right) \left(\sum_k \sigma_k^{t_1-1} \sigma_k^{t_2-1} \right)^{p-2} \frac{1}{(p-2)!} \right\} + 0 \left(N^3 \frac{(2-p)}{2} \right). \quad (3.17) \end{aligned}$$

The second order term may be exponentiated and δ -functions introduced to give

$$y = \exp \left[N \max_{q, r, k, s, m_1, n_1} Y(q, r, k, s, m_1, n_1) \right]$$

where

$$\begin{aligned} Y = \alpha \left[\sum_{t_1 < t_2} q^{t_1 t_2} r^{t_1 t_2} + \sum_{t_1, t_2} k^{t_1, t_2} s^{t_1 t_2} - \sum_{t_1 \neq t_2} p(p-1)(q^{t_1 t_2})^{p-2} s^{t_1 t_2} s^{t_2 t_1} - p(p-1) \sum_t (s^t)^2 \right] + \\ + i \sum_t n_1^{t-1} m_1^{t-1} + \ln \tilde{Y}(q, r, k, m_1, n_1) \quad (3.18) \end{aligned}$$

where,

$$\begin{aligned} \tilde{Y}(q, r, k, m_1, n_1) = \left\langle \text{Tr}_{\sigma_t} \int_0^\infty \frac{d\lambda^t}{2\pi} \int_{-\infty}^\infty dx^t \exp \left[i \sum_t x^t \lambda^t - i \sum_t p(m_1^{t-1})^{p-1} x^t \sigma^t \xi^1 - i \sum_t n_1^{t-1} \xi^1 \sigma^{t-1} - \right. \right. \\ \left. \left. - \alpha \sum_{i_1, i_2} k^{i_1 i_2} x^{i_1} \sigma^{i_1} \sigma^{i_2-1} - 2\alpha p \sum_{t_1 < t_2} x^{t_1} x^{t_2} \sigma^{t_1} \sigma^{t_2} (q^{t_1 t_2})^{p-1} - \alpha p \sum_t x_t^2 \right] \right\rangle_{\xi_1} \quad (3.19) \end{aligned}$$

All terms of higher order than the second in the expansion over microscopic patterns are of order $N^{\frac{2-p}{2}}$ relative to the second order term and therefore do not contribute in the thermodynamic limit. For $p = 2$ the whole series can be resummed to give the determinant $W(q, s, p)$ of equation (3.9c). The equation for m_1^1 after the first time step is then,

$$m_1^1 = 2 \operatorname{erf} \left(\frac{(m_1^0)^{p-1}}{\sqrt{2\alpha/p}} \right). \quad (3.20)$$

In contrast to the corresponding equation for the

Little model (3.14) the fixed point of the first stage of parallel interaction of the multiconnected model (3.19) are identical to the replica symmetric solution for the metastable state close to the pattern in the thermodynamic calculation [16]. There are two fixed points for $\alpha < \alpha_c(p)$ which approach one another as $\alpha \rightarrow \alpha_c(p)$ and the transition at α_c is first order.

4. Numerical study of long time behaviour.

In this section, we will first present numerical results obtained for the zero temperature parallel dynamics of the SK model. The calculations were done on

finite samples of N sites ($25 \leq N \leq 400$) and the quantities were averaged over 1 000 to 2 000 samples. The interactions J_{ij} were randomly chosen according to a flat probability $\rho(J_{ij})$ ($\rho(J_{ij}) = 1/2 J_0$ for $|J_{ij}| < J_0$ and $\rho(J_{ij}) = 0$ for $|J_{ij}| > J_0$). In the thermodynamic limit, all symmetric distributions of J_{ij} give the results which depend only on $\langle J_{ij}^2 \rangle$ for the SK model.

In table I, we give numerical results obtained for the magnetization $m(2)$, $m(4)$ and $m(\infty)$ at times $t = 2$, $t = 4$ and $t = \infty$ and for the overlap q^{42} and q^{53} . All these quantities except $m(\infty)$, describe the system after a few time steps and can be compared with the analytical results of section 2. We see that the agreement is excellent. One can also see in table I that the long time properties (like $m(\infty)$) depend much more on the size N than the short time properties.

In the approach developed in section 2, the calculations become more and more tedious as one increases the number of time steps. This makes the understanding of the long time behaviour quite difficult by this analytic approach. So for the long time behaviour, we could only use the numerical simulations. We have computed the magnetization $m_N(t)$ at the t -th time step (starting at $t = 0$ with $m_N(0) = 1$) and the correlation $q_N(t, t-2)$ between the configurations at time t and at time $t-2$ for samples of N spins. Due to gauge invariance, $q_N^{t, t-2}$ is independent of the starting configuration when it is averaged over disorder.

$$q_N(t, t-2) = \frac{1}{N} \sum_{i=1}^N \overline{\sigma_i(t) \sigma_i(t-2)}. \quad (4.1)$$

We did not consider $q(t, t-1)$ as it vanishes at all times equation (2.17). This is because for each i and t , $\sigma_i(t) \sigma_i(t-1)$ is an odd function of the interactions J_{ij} . One should notice that $q_N(t, t-2)$ defined

in (4.1) gives $q^{t+1, t-1}$ defined by (2.16) in the limit $N \rightarrow \infty$.

The remanent magnetization

$$m_N(\infty) = \lim_{t \rightarrow \infty} m_N(t)$$

depends strongly on the size N (Fig. 1) whereas at short times, the size dependence of $m_N(t)$ is much weaker. This makes the analysis of the long time behaviour of the magnetization rather difficult. The following two attempts were made :

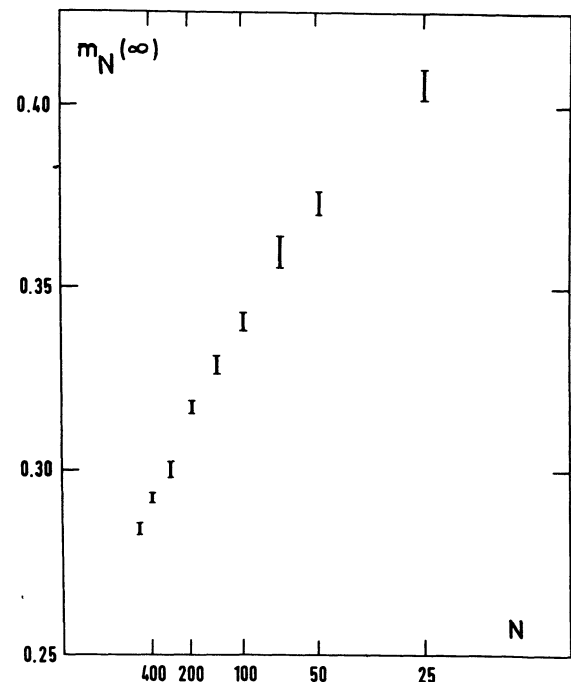


Fig. 1. — The magnetization $m_N(\infty)$ of the SK model versus $N^{-1/2}$. Extrapolating to $N \rightarrow \infty$ gives $m_\infty(\infty) = 0.23 \pm 0.02$.

Table I. — Magnetization at times 2, 4 and ∞ and the overlaps $q^{t, t-2}$ for $t = 4$ and 5 for the SK model. The results at short time converge quickly to the predictions of section 2. The convergence of $m(\infty)$ is much slower.

Size N	$m(2)$	$m(4)$	$m(\infty)$	q^{42}	q^{53}
—	—	—	—	—	—
25	0.5845 ± 0.0030	0.4748 ± 0.0035	0.4072 ± 0.0040	0.7571 ± 0.0025	0.8391 ± 0.0025
50	0.5813 ± 0.0020	0.4744 ± 0.0025	0.3738 ± 0.0030	0.7609 ± 0.0020	0.8353 ± 0.0015
100	0.5779 ± 0.0015	0.4719 ± 0.0015	0.3415 ± 0.0020	0.7581 ± 0.0012	0.8372 ± 0.0012
200	0.5767 ± 0.0010	0.4714 ± 0.0012	0.3177 ± 0.0015	0.7611 ± 0.0010	0.8364 ± 0.0008
400	0.5754 ± 0.0007	0.4686 ± 0.0008	0.2929 ± 0.0010	0.7603 ± 0.0006	0.8354 ± 0.0006
Results of section II	0.575	0.468		0.760	0.835

First, if one considers $m_N(t) - m_N(\infty)$ for each size N , the results seem to decay exponentially at long times

$$m_N(t) - m_N(\infty) \sim \exp - \frac{t}{\tau_N}. \quad (4.2)$$

Our numerical results suggest that τ_N increases like N^α where $\alpha \approx 0.5$. An accurate determination of α is not easy because we can only increase N up to a few hundreds and τ_N has to be extracted from the long time behaviour ($t > \tau_N$) for which the error bars are the biggest.

On the other hand, if we try to look at $m_\infty(t) - m_\infty(\infty)$, one finds a power law

$$m_\infty(t) - m_\infty(\infty) \sim t^{-\beta}. \quad (4.3)$$

The estimation of β is not easy either, because one needs to take the limit $N \rightarrow \infty$. For short times t , this is not very hard because $m_N(t)$ does not vary much with N but for $t \rightarrow \infty$, this is more difficult (see Table I and Fig. 1). Also the range of times on which the power law (3.3) can be observed is rather limited $1 \leq t \leq 20$ because our sizes N are small and (3.3) only be valid for $t < \tau_N$. However a log-log plot gives $0.5 \leq \beta \leq 0.7$ depending on what we choose for $m_N(\infty)$ versus $N^{-1/2}$. The convergence to $N \rightarrow \infty$ is rather slow and our estimate for $m_\infty(\infty)$ is

$$m_\infty(\infty) = 0.23 \pm 0.02. \quad (4.4)$$

The $N^{-1/2}$ convergence is the same as the one found by Kinzel for serial dynamics [7]. This value differs from $m_\infty(\infty) = 0.14 \pm 0.01$ predicted by Kinzel for sequential dynamics. This difference is not surprising because the two dynamics have no reason to give the same remanent magnetization. For example for 1d spin glasses, sequential dynamics give $m_\infty(\infty) = 1/3$ (see Ref. [12] and references therein) whereas parallel dynamics would give $m_\infty(\infty) = 2/3$. Also a value of $\beta \approx 0.5$ (see Eq. (3.3)) is rather similar to what had been previously found or predicted for finite temperature dynamics near the spin glass transition (Ref. [18] and references therein). It is not clear however whether our value of β could be compared with any result even at low temperature because one expects that $m_\infty(\infty) \neq 0$ for $T = 0$ whereas $m_\infty(\infty) = 0$ at low temperature.

The long time behaviour is much easier to study when one considers the time evolution of $q_N(t, t-2)$. In the limit $t \rightarrow \infty$, $q_N(t, t-2) \rightarrow 1$ independent of N . So the problem we had because of the N -dependence of the remanent magnetization is not present here. In figure 2 we show $\log(1 - q_N(t, t-2))$ versus $\log t$ for $N = 100$ and $N = 400$. We see for each size two regimes. The short time regime where

$$1 - q_N(t, t-2) \sim t^{-3/2} \quad (4.5)$$

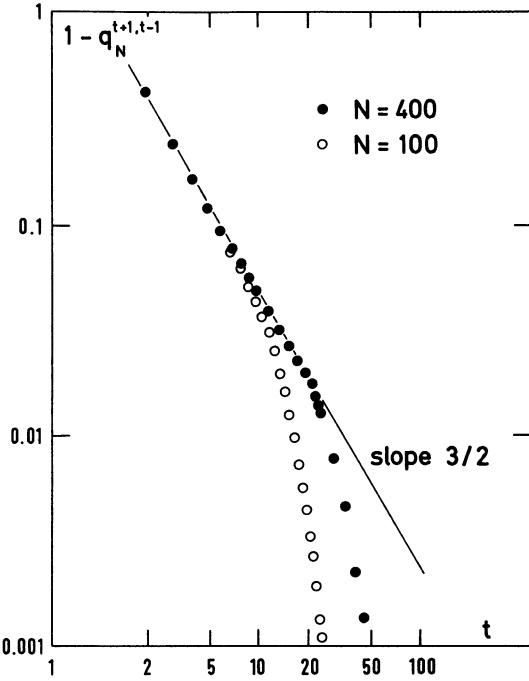


Fig. 2. — $1 - q_N^{t+1,t-1}$ versus t . The overlap $q_N^{t+1,t-1}$ is the overlap between a configuration at time t and at time $t-2$. We see that $1 - q_N^{t+1,t-1}$ decreases like $t^{-3/2}$ over a range of times which increases with N .

and a long time regime which is size dependent. The exponent $3/2$ is rather accurately determined. In figure 2 we see that, the range on which (4.5) holds increases with N and therefore (4.5) is probably valid at all times in the thermodynamic limit. The result (4.5) is compatible with the power law (4.3) and the estimate $0.5 \leq \beta \leq 0.7$ since one has always

$$\left| \frac{dm_N(t)}{dt} \right| \leq |1 - q_N(t, t-2)| \quad (4.6)$$

(3.6) expresses that the change in the magnetization is always less or equal to the number of spins which have flipped.

Another quantity which can be computed at short times analytically and at long times numerically is the overlap between two configurations. If one chooses 2 configurations $\{\sigma_i(0)\}$ and $\{\tau_i(0)\}$ at time $t = 0$, and if both configurations evolve according to the same set of interactions J_{ij} one can try to compute the time evolution of the overlap $Q(t)$

$$Q(t) = \frac{1}{N} \sum_{i=1}^N \sigma_i(t) \tau_i(t). \quad (4.7)$$

At short times, calculations very similar to those presented in section 2 give

$$Q(1) = \frac{4}{\pi} \tan^{-1} \left(\left(\frac{1+q}{1-q} \right)^{1/2} \right) - 1 \quad (4.8)$$

$$Q(2) = \frac{1+q}{2} f(q) - \frac{1-q}{2} f(-q) \quad (4.9)$$

where

$$f(q) = \int_{-\infty}^{+\infty} \int_{-\infty}^{+\infty} ds ds' \operatorname{sgn}(ss') \times \\ \times \frac{1}{4\pi\sqrt{a(1-a)}} \exp \left[- \left(\frac{s+s'}{2} - \sqrt{\frac{2}{\pi}} \right)^2 \frac{1}{2a} \right. \\ \left. - \left(\frac{s-s'}{2} \right)^2 \frac{1}{2(1-a)} \right]$$

where

$$a = \frac{2}{\pi} \tan^{-1} \left(\left(\frac{1+q}{1-q} \right)^{1/2} \right) \quad (4.10)$$

$$q = Q(0).$$

We see from these expressions that the calculation becomes more and more difficult as one increases the number of time steps and so here again, we could only study the long time behaviour by means of numerical simulations. In figure 3 we show $d(\infty)$ versus $d(0)$ for $0 \leq d(0) \leq 0.05$ where $d(t)$ is the

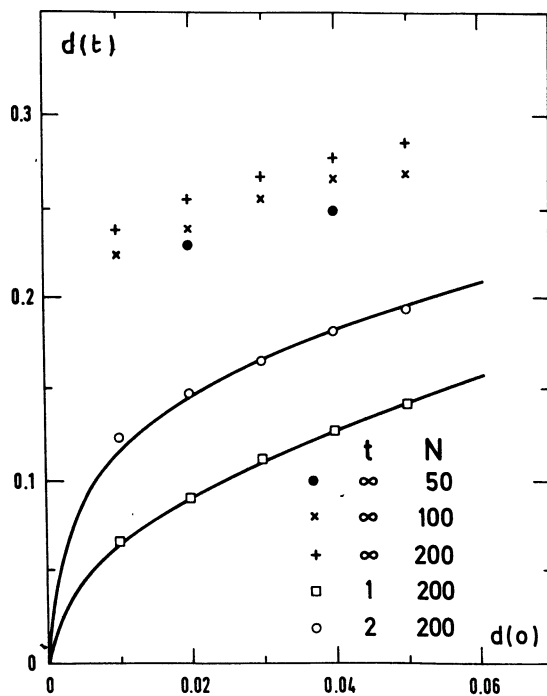


Fig. 3. — The distances $d(1)$, $d(2)$ and $d(\infty)$ at time $t = 1$, $t = 2$ and $t = \infty$ versus the initial distance $d(0)$ between two configurations for the SK model. The two curves are the result of equations (4.8)-(4.11). We see that $d(\infty)$ does not seem to vanish when $d(0) \rightarrow 0$.

distance between the two configurations and is defined by

$$d(t) = \frac{1 - Q(t)}{2} = \frac{1}{N} \sum_{i=1}^N \frac{(\sigma_i(t) - \tau_i(t))^2}{4}. \quad (4.11)$$

We see that, even $d(\infty)$ still depends on the system

size N , it is rather clear that $d(\infty)$ does not vanish when $d(0)$ vanishes

$$\lim_{d(0) \rightarrow 0} d(\infty) \approx 0.2$$

$$\text{or} \quad \lim_{Q(0) \rightarrow 1} Q(\infty) \approx 0.6.$$

It is not very easy to determine the limiting value accurately because one needs to take two limits, $Q(0) \rightarrow 1$ and $N \rightarrow \infty$. However, the fact that $d(\infty)$ does not vanish if $d(0) \rightarrow 0$ gives an idea of the structure of the basins of attraction of the attractors. Two starting configurations even if they are very close will evolve to attractors which are far apart.

This means that the frontiers, between basins of attraction are dense in phase space. Also this means that there is a cooperative effect between an infinite number of spins : if the dynamics could be reduced to finite clusters of spins, then when $d(0) \rightarrow 0$, the number of clusters for which the configurations $\sigma_i(0)$ and $\tau_i(0)$ differ would be proportional to $d(0)$. Only these clusters could contribute to $d(\infty)$ and therefore one would have $d(\infty)$ proportional to $d(0)$. The fact that $d(\infty)$ does not vanish as $d(\infty) \rightarrow 0$ means that there is a cooperative effect involving an infinite number of spins. The same results has already been found in the dynamics of other random systems : random networks of automata [17].

For the Little-Hopfield model, we have computed the overlap m_1^t with a stored pattern as a function of m_1^0 for several values of α . In figures 4, 5 and 6 we show our results for $\alpha = 0.1$, $\alpha = 0.4$ and $\alpha = 0.9$. For all these values of α , we observed that m_1^t has a limit m_1^∞ as $t \rightarrow \infty$. This means that the oscillations of m_1^t between odd and even times (which are present in the SK model) are either absent or too small to be observed (i.e. smaller than our error bar) for these values of α . We see that for $\alpha = 0.1$ (Fig. 4), the system remembers (since for $m_1^0 > 0.5$, one finds m_1^∞ very close to 1). It is interesting to notice that m_1^t is not always a monotonic function of time. For $\alpha = 0.4$, the system does not remember in the limit $t \rightarrow \infty$ ($m_1^\infty < m_1^0$). However for short times, we see that there is a range for which m_1^t and m_1^2 are larger than m_1^0 . This means that the configuration in the first time steps goes towards the pattern but at later times goes away. Lastly for $\alpha = 0.9$, we have always $m_1^t < m_1^0$ and the configuration always evolves away from the pattern.

There is therefore a qualitative difference between the results at long times and those for the first few time steps. For $\alpha < 0.64$ (0.67), the system remembers after 1 (2) time steps whereas at large time, the system remembers only if the initial overlap is

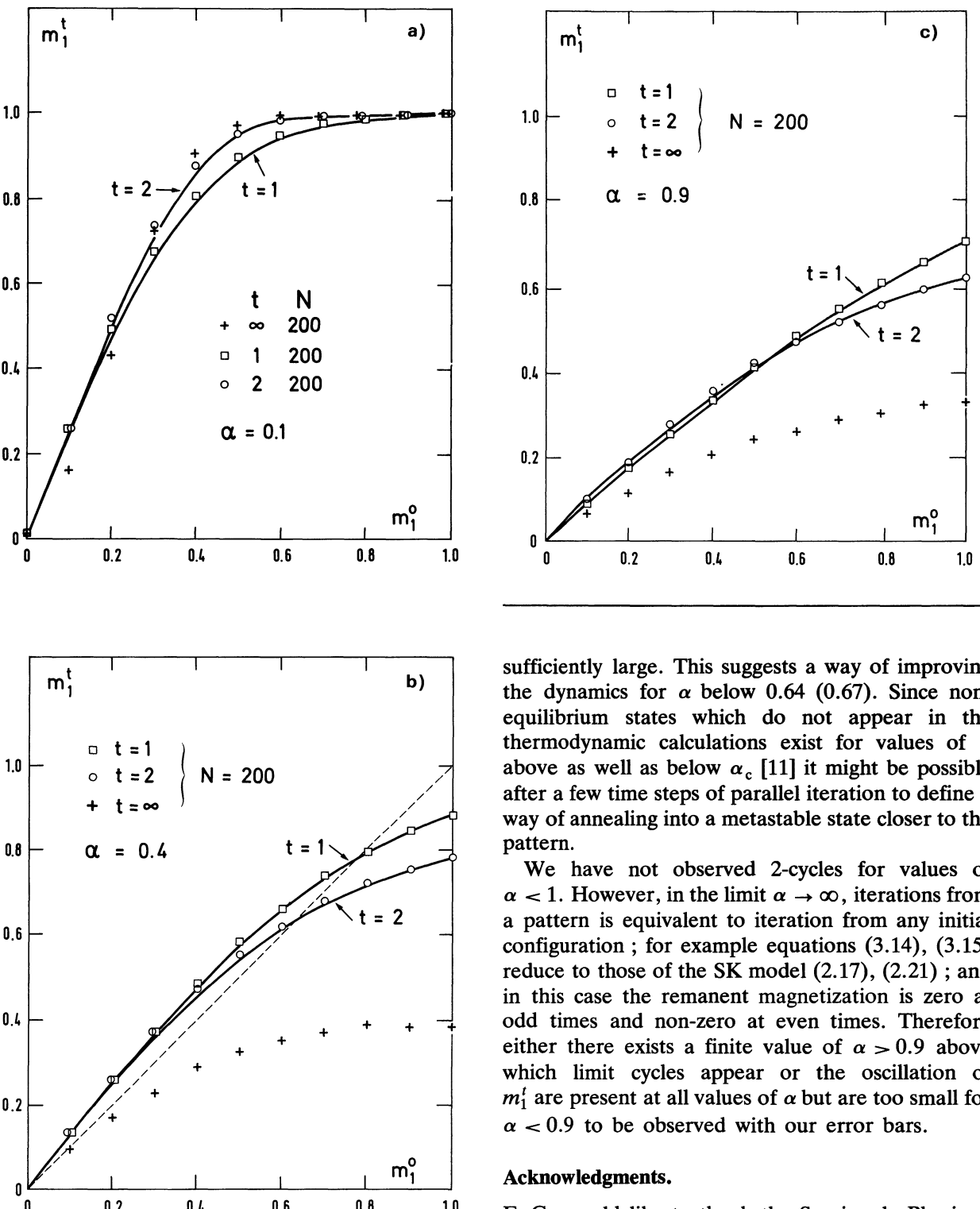


Fig. 4. — The overlap m_1^t for $t = 1, 2$ and ∞ with a stored pattern versus m_1^0 for the Little model : $\alpha = 0.1$ (Fig. 4a), $\alpha = 0.4$ (Fig. 4b), $\alpha = 0.9$ (Fig. 4c). The points are the results of numerical simulations and the curves were obtained from equations (3.14) and (3.15). For $\alpha = 0.1$ (Fig. 4a), the system learns. For $\alpha = 0.4$, the system goes towards the pattern for the first time steps if m_1^0 is small enough but does not learn in the long time limit (the dashed straight line is $m_1^t = m_1^0$). For $\alpha = 0.9$ (Fig. 4c) the system does not learn even in the finite time steps.

sufficiently large. This suggests a way of improving the dynamics for α below 0.64 (0.67). Since non-equilibrium states which do not appear in the thermodynamic calculations exist for values of α above as well as below α_c [11] it might be possible after a few time steps of parallel iteration to define a way of annealing into a metastable state closer to the pattern.

We have not observed 2-cycles for values of $\alpha < 1$. However, in the limit $\alpha \rightarrow \infty$, iterations from a pattern is equivalent to iteration from any initial configuration ; for example equations (3.14), (3.15) reduce to those of the SK model (2.17), (2.21) ; and in this case the remanent magnetization is zero at odd times and non-zero at even times. Therefore either there exists a finite value of $\alpha > 0.9$ above which limit cycles appear or the oscillation of m_1^t are present at all values of α but are too small for $\alpha < 0.9$ to be observed with our error bars.

Acknowledgments.

E. G. would like to thank the Service de Physique Théorique for their hospitality whilst visiting Saclay. Financial support for E. G. was from the Science and Engineering Research Council, U.K. and for P. M. from the Royal Society. Part of the work was done while B.D. was visiting the Institute of Theoretical Physics at Santa Barbara and was supported by the U.S. National Science Foundation under grant N° PHY 82-17853 supplemented by funds from the U.S. National Aeronautics and Space Administration.

Appendix 1.

In this appendix we show that any expectation value with respect to \tilde{y} , equations (2.13c), of the form

$$\langle x_T \sigma_T S(x_t, \sigma_t) \rangle_{\tilde{y}} = 0 \quad (\text{A.1})$$

in zero field where $S(x_t, \sigma_t)$ depends only on times earlier than T .

This expectation value contains a term of the form

$$I_T = \text{Tr}_{\sigma_T} \int_0^\infty d\lambda_T \int_{-\infty}^\infty \frac{dx_T}{2\pi} \sigma_T x_T \times \times \exp \left\{ ix_T \lambda_T - \frac{J^2}{2} x_T^2 + x_T \sigma_T C(x_t, \sigma_t) \right\} \quad (\text{A.2})$$

where

$$C(x_t, \sigma_t) = -J^2 \sum_{t=1}^{T-1} q^{Tt} x_t \sigma_t + iJ^2 r^T \sigma^{T-1} - i \sum_{t=1}^T s^{Tt} \sigma^{t-1}. \quad (\text{A.3})$$

Note that $C(x_t, \sigma_t)$ does not depend on x_T or σ_T . Taking the trace on σ^T gives

$$I_T = \int_0^\infty d\lambda_T \int_{-\infty}^\infty \frac{dx_T}{2\pi} x_T \times \times \exp \left(ix_T \lambda_T - \frac{J^2}{2} x_T^2 \right) (e^{x_T C} - e^{-x_T C}).$$

In the second term make the change of variable : $x_T \rightarrow -x_T$; $\lambda_T \rightarrow -\lambda_T$, so that

$$I_T = \int_{-\infty}^\infty d\lambda_T \int_{-\infty}^\infty \frac{dx_T}{2\pi} x_T \times \times \exp \left(ix_T \lambda_T - \frac{J^2}{2} x_T^2 + x_T C \right), \\ = \int_{-\infty}^\infty dx_T \delta(x_T) x_T \exp \left(-\frac{J^2}{2} x_T^2 + x_T C \right), \\ I_T = 0. \quad (\text{A.4})$$

Thus the expectation value, (A.1), is zero :

$$\langle x_T \sigma_T S(x_t, \sigma_t) \rangle_{\tilde{y}} = 0. \quad (\text{A.5})$$

Appendix 2.

In this appendix we give the results for the order parameters and magnetization up to 4 time steps, obtained from the saddle point equation (2.14a) for the SK model. The results up to $t = 2$ are given in equation (2.21), the remaining ones are :

$$s^{43} = \sqrt{\frac{2}{\pi}} e^{-(s^{32})^2/2} \left(1 - 2 \operatorname{erf} \left(\frac{q^{13} s^{32}}{\sqrt{1 - (q^{13})^2}} \right) \right)$$

$$s^{41} = \sqrt{\frac{2}{\pi}} 2 \operatorname{erf} \left(\frac{s^{32}}{\sqrt{1 - (q^{13})^2}} \right)$$

$$q^{42} = 2 \operatorname{erf} (s^{32}) + \frac{2}{\pi} \int_0^{\frac{q^{13}}{\sqrt{1 - (q^{13})^2}}} \frac{e^{-(1+a^2)(s^{32})^2/2}}{1+a^2} da$$

$$m(4) = q^{15} = 1 + \operatorname{erf} (s^{43} + s^{41}) - \operatorname{erf} (s^{43} - s^{41}) - \frac{1}{\pi} \left[\int_0^{\left(\frac{s^{43} + s^{41}}{s^{21}} - q^{24} \right) / \sqrt{1 - (q^{24})^2}} \frac{dw}{w^2 + 1} e^{-(w^2 + 1)(s^{21})^2/2} + \right.$$

$$+ \int_0^{\left(\frac{s^{43} - s^{41}}{s^{21}} + q^{24} \right) / \sqrt{1 - (q^{24})^2}} \frac{dw}{w^2 + 1} e^{-(w^2 + 1)(s^{21})^2/2} + \int_0^{\left(\frac{s^{21}}{s^{43} + s^{41}} - q^{24} \right) / \sqrt{1 - (q^{24})^2}} \frac{dw}{w^2 + 1} e^{-(w^2 + 1)(s^{41} + s^{43})^2/2}$$

$$+ \left. \int_0^{\left(\frac{s^{21}}{s^{43} - s^{41}} + q^{24} \right) / \sqrt{1 - (q^{24})^2}} \frac{dw}{w^2 + 1} e^{-(w^2 + 1)(s^{41} - s^{43})^2/2} \right]$$

$$q^{35} = \operatorname{erf} (s^{43} + s^{41}) + \operatorname{erf} (s^{43} - s^{41}) - \frac{1}{\pi} \left[\int_0^{\left(\frac{s^{43} + s^{41}}{s^{21}} - q^{24} \right) / \sqrt{1 - (q^{24})^2}} \frac{dw}{w^2 + 1} e^{-(w^2 + 1)(s^{21})^2/2} - \right.$$

$$- \int_0^{\left(\frac{s^{43} - s^{41}}{s^{21}} + q^{24} \right) / \sqrt{(1 - (q^{24})^2)}} \frac{dw}{w^2 + 1} e^{-(w^2 + 1)(s^{21})^2/2} + \int_0^{\left(\frac{s^{21}}{s^{43} - s^{41}} - q^{24} \right) / \sqrt{1 - (q^{24})^2}} \frac{dw}{w^2 + 1} e^{-(w^2 + 1)(s^{41} + s^{43})^2/2}$$

$$- \left. \int_0^{\left(\frac{s^{21}}{s^{43} - s^{41}} + q^{24} \right) / \sqrt{1 - (q^{24})^2}} \frac{dw}{w^2 + 1} e^{-(w^2 + 1)(s^{41} - s^{43})^2/2} \right]$$

$$s^{54} = \sqrt{\frac{2}{\pi}} e^{-(s^{43} + s^{41})^2/2} \left(\frac{1}{2} - \operatorname{erf} \left(\frac{s^{43} + (s^{41} - s^{21}) q^{24}}{\sqrt{1 - (q^{24})^2}} \right) \right) +$$

$$+ \sqrt{\frac{2}{\pi}} e^{-(s^{43} - s^{41})^2/2} \left(\frac{1}{2} - \operatorname{erf} \left(\frac{s^{43} - (s^{41} - s^{21}) q^{24}}{\sqrt{1 - (q^{24})^2}} \right) \right)$$

$$s^{52} = \sqrt{\frac{2}{\pi}} \left[\operatorname{erf} \left(\frac{s^{43} + s^{41} - s^{21} q^{24}}{\sqrt{1 - (q^{24})^2}} \right) + \operatorname{erf} \left(\frac{s^{43} - s^{41} + s^{21} q^{24}}{\sqrt{1 - (q^{24})^2}} \right) \right]$$

where $\operatorname{erf} x = \frac{1}{\sqrt{2 \pi}} \int_0^x dy e^{-y^2/2}$ and using the formula,

$$I(a, b, x) = \int_a^\infty d\mu \int_b^\infty d\lambda e^{-(\lambda^2 + \mu^2 + 2x\mu\lambda)/2} = J(a, b, x) + J(b, a, x)$$

where

$$J(a, b, x) = \int_{\frac{b}{a}+x}^\infty dz \frac{e^{-a^2(z^2 + 1 - x^2)/2}}{z^2 + 1 - x^2}.$$

References

- [1] BIENENSTOCK, E., FOGELMAN-SOULIÉ, F. and WEISBUCH, G., *Disordered Systems and Biological Organisation* (Springer Verlag, Heidelberg) 1986.
- [2] PARGA, N. and PARISI, G., preprint 85.
- [3] KANTER, I., SOMPOLINSKY, H., preprint 86.
- [4] WEISBUCH, G. and FOGELMAN-SOULIÉ, F., *J. Physique Lett.* **46** (1985) L-623.
- [5] FOGELMAN-SOULIÉ, F., GOLES-CHACC, E. and PELLEGRIN, D., *Discrete Applied Math.* 1984.
- [6] TANAKA, F. and EDWARDS, S. F., *J. Phys. F* **10** (1980) 2471.
DE DOMINICIS, C., GABAY, M., GAREL, T. and ORLAND, H., *J. Physique* **41** (1980) 923.
BRAY, A. J. and MOORE, M. A., *J. Phys. C* **14** (1981) 1313, *C* **13** (1980) L469.
- [7] KINZEL, W., *Phys. Rev. B* **33** (1986) 5086.
- [8] KIRKPATRICK, S., GELATT, C. D. and VECI, M. P., *Science* **220** (1983) 671.
- [9] AMIT, D. J., GUTFREUND, H. and SOMPOLINSKY, H., *Phys. Rev. A* **32** (1985) 1007 ; *Phys. Rev. Lett.* **55** (1985) 1530.
- [10] BRUCE, A. D., GARDNER, E. J. and WALLACE, D. J., *J. Phys. A* **20** to appear.
- [11] GARDNER, E., *J. Phys. A* **19** (1986) L1047.
- [12] DERRIDA, B. and GARDNER, E., *J. Physique* **47** (1986) 959.
- [13] SHERRINGTON, D. and KIRKPATRICK, S., *Phys. Rev. Lett.* **32** (1975) 1792.
- [14] LITTLE, W. A., *Math. Biosc.* **19** (1974) 101.
- [15] HOPFIELD, J. J., *Proc. Math. Acad. Sci.* **79** (1982) 2554.
- [16] GARDNER, E., *J. Phys. A* **20** to appear.
- [17] DERRIDA, B. and POMEAU, Y., *Europhys. Lett.* **1** (1986) 45.
- [18] SOMPOLINSKY, H. and ZIPPETIUS, A., *Phys. Rev. Lett.* **47** (1981) 359.
- [19] PERETTO, P., *Biol. Cybernet.* **50** (1984) 51.
- [20] FONTANARI, J. F. and KÖBERLE, R., São Carlos preprint (1986).